Subcritical transition to turbulence: What we can learn from the physics of glasses

Olivier Dauchot[1] and Eric Bertin[2]
[1]*EC2M, ESPCI-ParisTech, UMR Gulliver 7083 CNRS, 75005 Paris, France*
[2]*Université de Lyon, Laboratoire de Physique, ENS Lyon, CNRS, 46 Allée d'Italie, 69007 Lyon, France*
(Received 25 February 2012; revised manuscript received 3 August 2012; published 19 September 2012)

In this note, we discuss possible analogies between the subcritical transition to turbulence in shear flows and the glass transition in supercooled liquids. We briefly review recent experimental and numerical results, as well as theoretical proposals, and compare the difficulties arising in assessing the divergence of the turbulence lifetime in subcritical shear flow with that encountered for the relaxation time in the study of the glass transition. In order to go beyond the purely methodological similarities, we further elaborate on this analogy and propose a simple model for the transition to turbulence, inspired by the random energy model (a standard model for the glass transition), with the aim to possibly foster yet-unexplored directions of research in subcritical shear flows.

DOI: 10.1103/PhysRevE.86.036312 PACS number(s): 47.27.Cn, 47.27.eb, 64.70.P−

I. INTRODUCTION

Statistical physics has devoted a lot of effort to the study of fully developed turbulence, but much less to that of the transition to turbulence [1], which occurs when the Reynolds number, the ratio of the advection time to the viscous time, is increased. The transition is commonly observed in flow regimes lacking linear instability and is referred to as globally subcritical [2–4].

The plane Couette flow, driven by two plates moving parallel to each other in opposite directions, is linearly stable at all Reynolds numbers and, as such, is the epitome of globally subcritical transitions [5]. Other flows usually transit to turbulence before linear instability sets in. These include the circular Poiseuille flow (cPf) and the plane Poiseuille flow (pPf), which are driven by a pressure gradient respectively along a circular pipe or between two parallel plates, as well as the counter-rotating Taylor-Couette flow (TCf), driven by two concentric cylinders rotating in opposite directions. In all these cases, the transition is particularly delicate to understand due to its abrupt character. A complex spatiotemporal dynamics is observed, involving in particular the nucleation and the growth or decay of turbulent domains called "puffs" (pPf) or "spots" (pCf)—see, e.g., Refs. [6,7] for cPf, Refs. [8–10] for pCf, Ref. [11] for pPf, and Refs. [12,13] for TCf.

A recent surge of interest has been motivated by the audacious proposal that shear flow turbulence could remain transient up to arbitrarily large Reynolds numbers, opening ways towards a better control of such turbulent regimes [14]. This proposal was motivated by experimental and numerical observations in cPf [14] and pCf [15] regarding the statistics of turbulent lifetimes, which contradicted those previously obtained in cPf [16,17] and pCf [18,19]. These contradictory results, together with the experimental discovery of a spectacular long wavelength periodic organization of the laminar-turbulent coexistence in pCf and TCf [20,21], has motivated further experiments in TCf [22] and cPf [23,24], the development of various models [25–29], and an impressive number of numerical studies [23,30–41]. As a result, some comprehension of the mechanisms at play in the coexistence dynamics, as well as a better knowledge of the organization of phase space, involving many unstable solutions of the Navier-Stokes equation, has been gained.

Interestingly, the presence in phase space of many unstable solutions and the existence of finite, yet extremely large, relaxation times are reminiscent of the physics of glasses (see, e.g., Refs. [42–44]). In particular, whether the structural relaxation times of a glass really diverges at a given finite temperature or remains very large but finite at any positive temperature is an important question—related to the existence of a genuine phase transition to an ideal glass state—that remains largely open [45]. However, the intense activity related to this specific issue has triggered along the way different (and perhaps even more interesting) questions, driving the field of glasses towards important conceptual progress [44].

In this paper, we explore the analogy between the subcritical transition to turbulence and the glass transition from several viewpoints. After a concise review of the major results on the transition to turbulence, we discuss the limitations of fitting procedures in assessing the divergence of the turbulence lifetime, drawing inspiration from similar discussions in the glass literature (Sec. II). We then briefly review the theoretical scenarios and models that have been proposed to describe the subcritical transition to turbulence, and we tentatively discuss the analogy with glasses at a conceptual level (Sec. III). The understanding of the glass transition has greatly benefited from the study of oversimplified models like the random energy model [46,47], which describes the statistical behavior of a system evolving in a random energy landscape. In this spirit, we try to transpose the random energy model, keeping in mind both its strengths and weaknesses, to the modeling of the subcritical transition to turbulence, in order to possibly gain insight into the statistical mechanisms at play in this transition (Sec. IV). As a result, we obtain an estimate of the turbulence lifetime as a function of the Reynolds number close to the transition, an estimate which qualitatively agrees amazingly well with the observed phenomenology.

Clearly, this qualitative agreement does not in itself prove the analogy to be specifically deep, but it suggests that it deserves to be further explored. More generally, we hope, in the spirit of Pomeau's seminal paper [48], that the analogy presented here could foster contributions from the statistical physics community to the old standing problem of the transition to turbulence, taking advantage of recently developed concepts in the statistical physics of disordered

systems. Conversely, the development of techniques such as particle image velocimetry and the exponential increase of the numerical capacities could help in validating or invalidating the assumptions made on some properties of turbulence in following the present analogy.

II. TURBULENCE LIFETIME

A. A review of experimental and numerical observations

A standard characterization of the subcritical transition to turbulence is the determination of the average turbulence lifetime, following either a perturbation or a quench, as a function of the Reynolds number. We thus start by briefly reviewing the experiments and direct numerical simulations reporting the increase of the turbulence lifetime when the Reynolds number is increased. To our knowledge, the first systematic measurement of turbulence lifetimes was conducted in the pCf [18,19]. Two different kinds of experiments have been performed, differing by the way the initial condition is prepared. In what we shall call type-A experiments, the Reynolds number, R, is set to its value of interest and the laminar flow is disturbed locally at the initial time. In type-B experiments, a turbulent flow is prepared at high R and quenched at the initial time down to the R value of interest. In both cases, one monitors the evolution of the turbulent fraction $f_T(t)$, which characterizes the coexistence dynamics of laminar and turbulent domains (see Fig. 1). For $R > R_g$, $f_T(t)$ fluctuates around some average value, which remains finite on experimental time scales. For $R < R_u$, $f_T(t)$ relaxes towards zero, without displaying any long transient regime. In between, for $R_u < R < R_g$, $f_T(t)$ exhibits a, first, rapid decay, followed by a long transient quasisteady regime, before a large fluctuation sets it to zero. The lifetime of these transients are exponentially distributed and the average value τ was reported to diverge like $(R_g - R)^{-1}$.

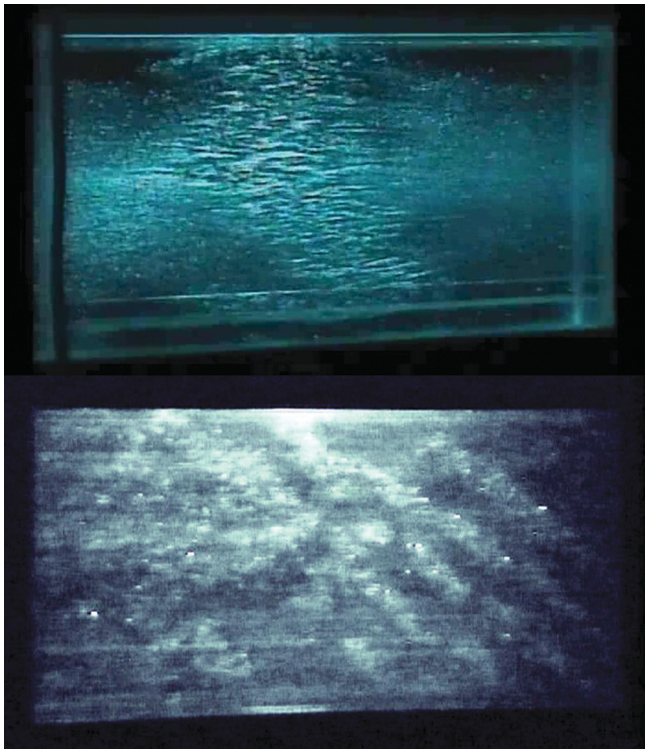

FIG. 1. (Color online) Typical snapshots of the laminar-turbulence coexistence at intermediate Reynolds number in plane Couette flow. (Top) Turbulent spot in a small aspect ratio setup, created by a localized perturbation. (Bottom) Large-scale coexistence in a large aspect ratio setup, following a quench from high Reynolds number.

The cPf was later investigated in various ways. In Refs. [6,17] a puff was generated inside a constant flow rate pipe flow by introducing a short duration perturbation. Then R was reduced and the subsequent evolution of the puff was monitored as it progressed downstream. The probability of observing a localized disturbed region of flow as a function of distance downstream is exponential and the time required for half of the initial states to decay, $\tau_{1/2}$, was reported to diverge like $(R_c - R)^{-1}$, in agreement with the observations made in the pCf. Other protocols lead to the same conclusions [6,17].

However, these results were challenged later by another experimental study [14]. In a pressure driven flow through a very long pipe, the authors could record much longer dimensionless observation times. They could determine the probability to be turbulent after a time period given by the distance between the perturbation location and the outlet, as a function of flow rate. For short times, the data are within the error bars of Refs. [6,17] but, for longer times, they deviate from the divergent behavior reported above and are better represented by an exponential variation, $\tau = \exp(aR + b)$, without singularity (here and in what follows, a and b denote generic fit parameters). Finally, in a recent experimental study of turbulence in pipe flow spanning height orders of magnitude in time, drastically extending all previous investigations, it was claimed that the turbulent state remains transient, with a mean lifetime, which depends superexponentially on the Reynolds number: $\tau \propto \exp[\exp(aR + b)]$ [49].

Intense numerical simulations of the cPf have also been conducted but did not clarify the situation. In Refs. [16,31] a diverging behavior of the turbulent lifetimes compatible with the experimental results of Refs. [6,17] is reported. Later in Ref. [32], the authors—one of which is common to Ref. [16]—conducted further simulations and reanalyzed older data, concluding to an exponential dependence such as the one reported in Ref. [14]. Altogether despite intense experimental and numerical effort, no definitive answer regarding the divergence or finiteness of turbulence lifetime could be obtained from the fit of data by phenomenological functional forms.

B. Fitting procedures: Lessons from glass physics

As stated in the Introduction, this issue is not specific to the transition to turbulence. When a liquid is suddenly quenched below its crystallization temperature and if crystallization can be avoided, the liquid enters a state, called supercooled liquid, in which the relaxation time increases by several orders of magnitude over a limited range of temperature [42]. A divergence at a finite temperature of the relaxation time would signal an ideal glass transition and, thus, would be of high interest, at least at a conceptual level. Despite huge efforts made to measure the variations of the relaxation time over

an experimental window of more than 10 decades, no clear consensus has been obtained yet. More precisely, the available data are both consistent with fits including a divergence at a finite temperature $T_c > 0$ and with fits diverging only at $T = 0$ [45].

The same difficulty is also expected to appear in the context of turbulence. We illustrate this point on experimental data recently obtained in the case of the TCf [22], when only the external cylinder is rotating. The TCf is then, like the pCf, linearly stable for all R. Also, because the TCf is a closed flow, one can record very long times. In this experiment, the angular rotation of the external cylinders fixes the Reynolds number. The flow was perturbed by rapidly accelerating the inner cylinder in the direction opposite to the rotation of the outer cylinder and immediately stopping it. After a short regime of featureless turbulence, the flow exhibits long transients characterized by the coexistence of laminar and turbulent domains, before eventually relaxing towards the laminar flow. The distribution of lifetimes is again exponential, and the authors argue that the mean turbulent lifetime does not diverge and rather behaves in the transitional regime as a double exponential $\tau \propto \exp[\exp(aR + b)]$, as observed in the cPf [49].

It is interesting to note that in the oldest experiments, the debate about the functional dependence of the average turbulent lifetime on the Reynolds number was concentrating on the choice between the two following forms:

$$\tau/\tau_0 = \exp(R/R_0), \tag{1}$$

$$\tau/\tau_0 = \left(\frac{R_c}{R_c - R}\right)^{\alpha}, \quad \alpha > 0, \tag{2}$$

whereas the most recent experiments, both in the case of the cPf [49] and the TCf [22], have access to much longer experimental time scales and point at a double exponential behavior. This last functional form ensures a very fast increase of τ without singularity and could give the impression that it solves the above debate. However, as learned from the physics of glasses, the debate has actually been shifted towards two alternative functional forms, namely

$$\ln(\tau/\tau_0) = \lambda \exp(R/R_0), \tag{3}$$

$$\ln(\tau/\tau_0) = \lambda \left(\frac{R_c}{R_c - R}\right)^{\alpha}, \quad \alpha > 0. \tag{4}$$

As a matter of fact, Eq. (4), which has (to the best of our knowledge) not yet been proposed in the context of the transition to turbulence, is a very standard form called the Vogel-Fulcher-Tammann (VFT) law in the physics of glasses [45].

Figure 2 displays the data obtained in TCf [22]—which are available online as Supplementary Material of Ref. [22] with that paper—together with possible fits by the four functional forms proposed above. Note that we have only performed global fits of the data, without trying to extract various regimes and crossovers as can be done in the case of glasses [45]. One clearly observes that, indeed, the relevant variable to describe the growth of the turbulent lifetimes is $\ln(\tau)$, as soon as really large times are considered. However, one also sees that apart from the simple exponential form Eq. (1), all other descriptions are not discriminable, so there is no definitive way

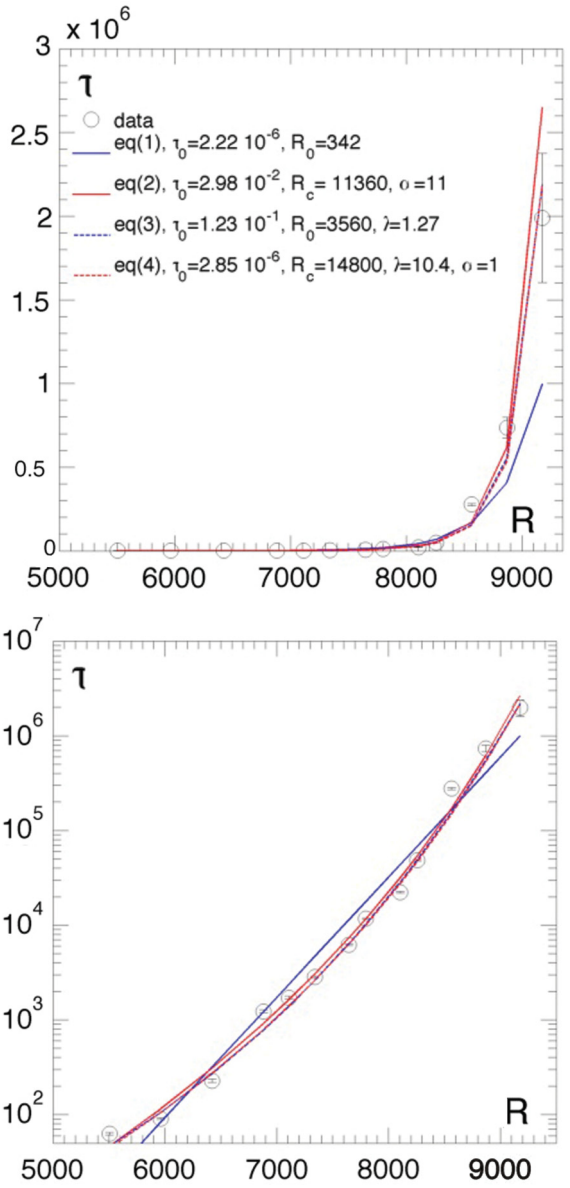

FIG. 2. (Color online) Probing finite lifetime experimentally: Relaxation lifetimes of turbulent initial conditions in a Taylor-Couette flow, with rotating external cylinder and internal cylinder at rest (data from Ref. [22]). Four possible fits are proposed as indicated in legend. Top and bottom panels are in lin-lin and lin-log scales respectively. Times are given in units of $d/r_0\omega_0$, where d is the gap between the two cylinders, r_0 is the radius of the external cylinder and ω_0 its angular velocity. All fits were performed using a standard least-squares fit procedure. Fit with Eq. (1) (lowest curve on top panel and straight line on bottom panel) was obtained by imposing a linear fit of $\log(\tau)$ vs. R. Fit with Eq. (2) (highest curve on top panel and convex curve on bottom panel) was obtained by imposing a linear fit of $\log(\tau)$ vs. $\log(R_c/(R_c - R))$, optimizing the fit quality on R_c. Fit with Eq. (3) ((dotted line, undistinguishable from fit with Eq (4)) was obtained by imposing a linear fit on $\log(\tau)$ vs. $\exp(R/R_0)$, optimizing the fit quality on R_0. Finally, fit with Eq. (4) [dotted line, undistinguishable from fit with Eq (3)] was obtained by imposing a linear fit of $\log(\tau)$ vs. $R_c/(R_c - R)$, optimizing the fit quality on R_c. In this last case, α was, thus, set to 1. It was checked that other values of α up to 3 cannot be discriminated. For Eq. (1), the regression coefficient r_2 is equal to 0.971. For all the other cases, $r_2 = 0.994$.

to rule out or confirm the existence of a singularity. One faces the same difficulty as in the physics of glasses: the lifetimes to be measured become very large, which makes it difficult to accumulate significant statistics. The experimental results are thereby confined to a finite range of Reynolds number or temperature, from which even with high-quality data sets, the divergence of a characteristic time cannot convincingly be determined from fits.

Before concluding this section, let us mention that the double-exponential form [Eq. (3)] has been justified on the basis of extreme value statistics [50]. However, as stated by the authors, the argument is only local, as it involves an expansion in R around a given reference value. Hence, no clear conclusion can be drawn from the theoretical argument of Ref. [50] on the issue of the divergence of τ at a finite or infinite value of R. Finally, let us emphasize that, for now, we have left aside all issues related to finite-size effects, which in turn can severely alter the functional dependence of time and length scales in transitional regimes.

III. THEORETICAL SCENARIOS AND MODELS

After discussing the empirical results, a natural question is to know how one can understand, from a more theoretical perspective, the globally subcritical transition to turbulence. This transition is by definition controlled by solutions of the Navier-Stokes equation, which do not branch continuously from the laminar flow solution when the Reynolds number is increased [51]. These solutions—of various kinds, stationary states, traveling waves, or more complex coherent structures—are unstable and form hyperbolic states, with stable and unstable manifolds. Early indications of the existence of these solutions were reported in pCf, both numerically [52–54] and experimentally [55]. More recently, they were also observed in the cPf [56]. The intricate network made of these manifolds and their connections then serves as a skeleton for the turbulent flow.

A. Low-dimensional models

In principle, one would like to collect all such states, estimate their dynamical weight, and calculate statistical averages from periodic orbit theory [57]. In practice, one must restrict the analysis to low-dimensional models [58–63] or to simulations [14,16,25,32,62,64–66], performed in the so-called minimal flow unit assumption [67]. Doing so, it was shown that the regions of initial conditions for which long lifetimes exhibit strong fluctuations and a sensitive dependence on initial conditions were separated from the regions with short lifetimes and smooth variations by a border, the so-called "edge of chaos" [62,63,65]. Later, some exact solutions with codimension-1 stable manifolds have been identified as edge states, that is, solutions that locally form the stability boundary between laminar and turbulent dynamics [35–37,68]. These important results contributed to make concrete the picture borrowed from dynamical system theory of a turbulent repellor, separated from the laminar state by a set of edge states connected through heteroclinic manifolds. In particular, the existence of the above nontrivial solutions has served to understand the exponential distribution of lifetimes in the transitional regime.

B. Spatially extended models

Unfortunately the above picture does not bring a complete description of the subcritical transition to turbulence. As argued in Refs. [26,28,69], the reason is that the dynamics, being either projected on a small set of modes or limited to small computational domains with periodic boundary conditions, cannot capture the genuinely spatiotemporal coexistence of laminar and turbulent states observed in open and unbounded flows. In particular, it can neither capture the long wavelength modulation of turbulent intensity nor the regime of alternating laminar and turbulent stripes, first observed experimentally in pCf and TCf [20,21], and then reproduced numerically in pCf [30,34,37,39,41,70].

As a matter of fact, it has long been known that, according to the scenario called spatiotemporal intermittency [71], transient chaotic states locally distributed in space, e.g., on a lattice, may evolve into a sustained turbulent global state due to spatial couplings [72–75]. Following this path, it was demonstrated that a simple 1D model of cPf, composed of coupled maps, does indeed capture remarkably well the character of the turbulent pipe flow in the transitional regime and exhibits a critical transition towards sustained turbulence via spatiotemporal intermittency [29]. The transition is further believed to belong to the directed percolation class [72,73,76], as already suggested in Ref. [48] for pCf, and recently reconsidered in cPf [77].

Finally, it was shown by means of fully resolved direct numerical simulations of the Navier Stokes equation that there exists a crossover length scale of the order of 10^2 times the cross-stream length below which the spatiotemporal processes at play in large-scale simulations and experiments are not captured [28]. Since then, a number of numerical investigations of large aspect ratios cPf and pCf have reproduced the complex spatiotemporal coexistence of laminar and turbulent states and identified the first hydrodynamics mechanisms at play [23,37,38,41].

C. Analogies and differences with glasses

We now wish to discuss from a theoretical perspective the analogies, as well as the differences, between flows close to the transition to turbulence (in short, transitional flows) and liquids close to the glass transition. To this aim, it is useful to, first, summarize the essential features of the subcritical transition to turbulence.

(a) *Subcriticality*: While the laminar flow is stable against infinitesimal perturbations, finite amplitude perturbations may trigger an abrupt transition towards a disordered flow. Such a disordered flow can also be obtained by quenching fully turbulent flows.

(b) *Spatiotemporal intermittency*: This disordered flow is made of turbulent domains, which move, grow, decay, split, and merge, leading to spatiotemporal intermittency, that is, a coexistence dynamics in which active or turbulent regions may invade absorbing or laminar ones, where turbulence cannot emerge spontaneously.

(c) *Transients and metastability*: For large-enough Reynolds numbers, this disordered flow has long lifetimes, which are distributed exponentially. Whether the associated characteristic time diverges at a finite Reynolds number is still a matter of debate. For low Reynolds numbers, say $R < R_u$, or small-enough disturbances, the flow relaxes rapidly towards the laminar flow.

(d) *Unstable states*: When increasing the Reynolds number a larger and larger number of unstable finite amplitude solutions appear in phase space. Some have been identified as edge states separating the others from the laminar state.

As mentioned in the Introduction, some of these features are also shared, at a qualitative level, with glasses. For instance, the presence of long transient relaxing states is a key feature of glasses [42]. Also, the existence of many unstable solutions is reminiscent of the energy landscape picture of glasses [78]. Indeed, the slow relaxation in glasses has been argued to result from the wandering of the phase-space point representing the system in a complex energy landscape [79], mostly composed of many unstable fixed points [43,80,81] (though local minima also play an important role at low-enough temperatures). The most striking feature of the glass transition, the rapid increase of the relaxation time by several orders of magnitude over a moderate range of temperatures, is also interpreted as a consequence of this complex dynamics in phase space. These results from glass theory suggest that the complex structure of phase space in transitional flows, with the presence of many unstable solutions, plays an important role in the properties of the subcritical transition to turbulence. To elaborate on this idea, we propose in the next section an extension of the simplest model of the glass transition, namely the random energy model [46,47], to the context of the transition to turbulence.

Other possible similarities between the transition to turbulence and the glass transition can be pointed out, considering now the real-space dynamics. For instance, one of the recurrent feature of glassy systems is the heterogeneities of the dynamics: slowly and rapidly relaxing regions coexist in real space, permanently evolving in a complex spatiotemporal organization [82]. This is reminiscent of the dynamics observed in subcritical transitional flows, where regions with different level of fluctuations coexist. And indeed, some of the one-dimensional models introduced to describe such dynamical heterogeneities in glasses, the so-called kinetically constrained model [83,84] exhibit spatiotemporal dynamics which are very similar to those observed in the one-dimensional models introduced to discuss the transition via spatiotemporal intermittency [29,73], especially when looking at spatiotemporal diagrams. For some of the KCM models, the critical point observed in the limit of zero temperature even belongs to the directed percolation class.

Let us emphasize that beyond the possible analogies discussed above, there are also many important differences between the glass transition and the transition to turbulence. A first difference is that supercooled liquids, in which the relaxation time strongly increases when lowering temperature close to the glass transition, are equilibrium systems, while transitional flows are intrinsically nonequilibrium systems. Indeed, the control parameter of the transition (the Reynolds number) may be thought of as a distance to equilibrium, which has to be increased to reach the turbulent state. Another difference is that the turbulent lifetime is the time before the flow falls into the absorbing laminar state, while the relaxation time in glasses is defined from the relaxation of density, or stress, correlations; no absorbing state is involved in this case.

A precise mapping between the glass transition and the transition to turbulence thus should not be expected, and the proposed analogy should not be considered in a strict sense. As we shall see now, there is, for instance, no direct mapping between, say, the Reynolds number and the temperature. The idea underlying the present work is, rather, to take advantage of the methodological and conceptual tools developed in the framework of the glass transition to shed some light on the subcritical transition to turbulence, keeping in mind the limitations of such an approach. Still, we shall see, as a first illustration, that it allows us to discuss in an original way the dependence of the turbulence lifetime on the Reynolds number.

IV. A RANDOM ENERGY MODEL FOR TRANSITIONAL FLOWS

Along the lines described in the last section, we now introduce a simple model that captures, as an essential ingredient, the wandering of the system on a complex landscape. This model is a variant of the random energy model [46,47], a toy model which has proved useful in the understanding of the glass transition, in spite of its oversimplified character. As a by-product, our model yields interesting predictions for the dependence of the turbulent lifetime on the Reynolds number, as discussed below.

A. Diffusion in the energy landscape

As a first step, it is necessary to statistically characterize the properties of the energy landscape, in particular, the number of unstable solution at a given energy above the laminar state, as function of the Reynolds number and of the volume of the flow. Though numerical investigations of turbulent flows have not been able yet to characterize the number of unstable solutions as a function of the volume of the flow, the analogy with glasses suggests that this number of solutions may grow exponentially with the volume of the system. Characterizing the state of the flow by its turbulent energy per unit volume, $\varepsilon = E/V$ (that is, the excess kinetic energy with respect to the laminar flow), we assume that the number $\Omega_V(\varepsilon, R)$ of unstable solutions at a given energy density ε and Reynolds number R grows exponentially with the volume V according to

$$\Omega_V(\varepsilon, R) \sim e^{V s(\varepsilon, R)}, \tag{5}$$

thus defining an entropy density $s(\varepsilon, R)$. At low Reynolds number, no unstable states exist, so we assume that the entropy $s(\varepsilon, R)$ is equal to zero for all $\varepsilon > 0$ if R is less than a characteristic value R_u. For $R > R_u$, we assume that $s(\varepsilon, R) > 0$ on an interval $\varepsilon_{\min}(R) < \varepsilon < \varepsilon_{\max}(R)$, and $s(\varepsilon, R) = 0$ otherwise, meaning that unstable states exist only in the energy interval $(\varepsilon_{\min}, \varepsilon_{\max})$.

Turning to dynamics, we assume, on the basis of the experimental and numerical observations reported in Sec. III, that the turbulent flow spends most of its time close to unstable solutions and that the evolution of the flow can be considered as a succession of jumps between different unstable solutions. If, however, the flow ends up in the laminar state,

the evolution stops until an external perturbation is imposed. Taking into account the presence of the absorbing laminar state is obviously essential to determine the lifetime of the turbulent flow. This will be the focus of Sec. IV B. Yet, in a first stage, it is interesting to consider the evolution of the turbulent flow in the absence of the absorbing laminar state, in order to make the analogy with glass models emerge more clearly.

As it is unlikely that a large amount of energy could be injected or dissipated within a short time period, one expects that the energy of successively visited unstable solutions are close to one another. At a coarse-grained level, it is then natural to assume that the energy ε evolves diffusively. In order to take into account the variation with ε of the number of unstable states, the evolution should also be biased toward values of the energy with a high entropy $s(\varepsilon,R)$. More precisely, the bias should depend on the derivative of the entropy with respect to the energy (a constant entropy introduces no bias in the dynamics). Altogether, the simplest evolution equation for the energy $\varepsilon(t)$ incorporating the above ingredients is the following Langevin equation

$$\frac{d\varepsilon}{dt} = \gamma s'(\varepsilon,R) - \lambda + \xi(t), \tag{6}$$

where the prime denotes a derivative with respect to ε. To enforce the finite range of values $\varepsilon_{\min} < \varepsilon < \varepsilon_{\max}$, reflecting boundary conditions are assumed at $\varepsilon_{\min}$ and $\varepsilon_{\max}$. The parameter γ is a proportionality coefficient to be determined later on, included for dimensional reasons. The term λ accounts for dissipative effects, and $\xi(t)$ is a white noise describing the energy injection mechanism, satisfying

$$\langle \xi(t)\xi(t')\rangle = 2D\,\delta(t-t'), \tag{7}$$

where D is a diffusion coefficient in energy space. These are obviously strong simplifications: the dissipation rate could, in principle, depend on ε and the noise should rather be considered as colored and multiplicative in such nonequilibrium systems, but we wish to keep the model as simple as possible for the sake of illustration. The assumption of a constant dissipation rate is, however, justified in the limit where the width $\varepsilon_{\max} - \varepsilon_{\min}$ of the accessible energy range is small with respect to $\varepsilon_{\min}$. Besides, considering that the noise is self-generated by the turbulent fluctuations, and, thus, results from the superposition of a number of contributions proportional to the volume V, one expects the diffusion coefficient to scale as $D = D_0/V$. Note that all parameters γ, λ, and D_0 may depend on the Reynolds number R.

The Fokker-Planck equation describing the evolution of the probability distribution $P(\varepsilon,R,t)$ then reads

$$\frac{\partial P}{\partial t} = -\frac{\partial}{\partial \varepsilon}([\gamma s' - \lambda]\,P) + \frac{D_0}{V}\frac{\partial^2 P}{\partial \varepsilon^2}. \tag{8}$$

The stationary solution $P(\varepsilon,R)$ is obtained as

$$P(\varepsilon,R) = \frac{1}{Z}\exp\left\{\frac{V}{D_0}[\gamma s(\varepsilon,R) - \lambda\varepsilon]\right\}. \tag{9}$$

Following standard statistical physics arguments, one expects the distribution $P(\varepsilon,R)$ to be proportional to the number of unstable states $\Omega_V(\varepsilon,R) \sim e^{Vs(\varepsilon,R)}$, which imposes $\gamma = D_0$. Introducing the parameter $\beta = \lambda/D_0$, the stationary distribution then reads

$$P(\varepsilon,R) = \frac{1}{Z}\exp\{V[s(\varepsilon,R) - \beta(R)\varepsilon]\}, \tag{10}$$

where we have emphasized the R dependence of the parameter β, which, in the present context, describes the balance between the energy injection and the dissipation, as does the inverse temperature at equilibrium. If V is large, the distribution is dominated by the energy $\bar{\varepsilon}(R)$ which maximizes the argument of the exponential, namely $s(\varepsilon,R) - \beta(R)\varepsilon$. If the maximum of $s(\varepsilon,R) - \beta(R)\varepsilon$ lies within the interval $\varepsilon_{\min}(R) < \varepsilon < \varepsilon_{\max}(R)$, the most probable energy is the solution of

$$s'(\bar{\varepsilon}(R),R) - \beta(R) = 0. \tag{11}$$

Assuming the entropy $s(\varepsilon,R)$ to be a concave function of ε (see Fig. 3), $s'(\varepsilon,R)$ is a decreasing function of ε and, thus, has its maximum at $\varepsilon = \varepsilon_{\min}(R)$.

We now introduce the key element of the model, which we borrow from the random energy model [46,47]. The specificity of the latter, which leads to a glass transition, is that the entropy has a finite slope at the minimum energy. By analogy, we thus assume that $s'(\varepsilon,R)$ takes a finite value, denoted as $\beta_0(R)$, when $\varepsilon \to \varepsilon_{\min}(R)$.

From a statistical physics point of view, the presence of a finite slope of the entropy at the minimum energy is related to the presence of long-range interactions in the system. Indeed, one can check that for short-range interacting systems, the entropy has an infinite slope at the minimal energy [85]. In the random energy model, the fact that all energy levels are statistically independent implicitly results from long-range (mean-field type) interactions. Indeed, the random energy

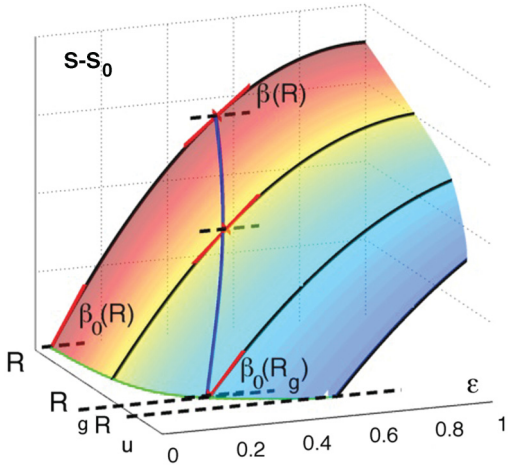

FIG. 3. (Color online) Sketch of the entropy surface and its slopes along the energy density direction, together with the path followed by the flow while varying the Reynolds number. Colors of the surface go from blue to red with increasing Reynolds number ($R_g > R_u$). The green line, on the plane $s - s_0 = 0$ indicates $\varepsilon_{\min}(R)$. Fixing some Reynolds number R (here a given black line among the four drawn on the entropy surface) one sets $\beta(R)$. Solving Eq. (11) then graphically amounts to finding a slope along the energy density direction equal to $\beta(R)$. A solution exists if $\beta(R) < \beta_0(R)$, the slope at the intersect with $\varepsilon_{\min}(R)$. Varying R, one follows the blue path on the surface (here the line intersects three black lines), eventually leading to the value R_g such that $\beta(R_g) = \beta_0(R_g)$.

model can be interpreted as the limit of mean-field spin-glass models where interactions involve p spins (instead of two spins for, e.g., the Ising model), when $p \to \infty$ [47].

In the context of the subcritical transition to turbulence, the presence of the pressure field and of large-scale unstable solutions, such as the unstable longitudinal vortices, naturally induces such long-range correlations. Note also that long-range correlations are well known to be present in the fully turbulent regime, as seen, for instance, by the presence of non-Gaussian fluctuations in the flow [86,87]. The generic presence of long-range correlations in turbulent flows thus make plausible the assumption of a finite slope of the entropy at the minimal energy where unstable solutions exists. Clearly, this hypothesis would need to be checked in numerical simulations of realistic flows, which is, however, a complicated task. We thus presently take this assumption as a working hypothesis motivated by the analogy with glasses and explore its consequences in the framework of subcritical turbulence modeling.

Coming back to the model, we see that if $\beta(R) < \beta_0(R)$, Eq. (11) generally admits a solution $\bar{\varepsilon}(R) > \varepsilon_{\min}(R)$. In contrast, if $\beta(R) > \beta_0(R)$, Eq. (11) has no solution, and $s(\varepsilon, R) - \beta(R)\varepsilon$ is maximum at $\varepsilon = \varepsilon_{\min}(R)$. The probability distribution then concentrates on $\varepsilon_{\min}(R)$. Intuitively, one expects $\beta(R)$ to be a decreasing function of R (that is, the temperature β^{-1} characterizing the fluctuations increase with the Reynolds number). On the other hand, the total number of unstable states increases with the Reynolds number, and it is thus plausible that $\beta_0(R)$ increases (or at least remains constant) with R. This suggests the existence of a Reynolds number R_g such that $\beta(R_g) = \beta_0(R_g)$. In this case, the average energy $\bar{\varepsilon}(R)$ is larger than $\varepsilon_{\min}(R)$ for $R > R_g$, while the dynamics in phase space concentrates on the states of minimal energy for $R < R_g$.

As emphasized at the beginning of this section, these conclusions hold under the unphysical hypothesis that no laminar state is present. However, if the paths leading from the unstable states to the laminar one are rare enough, the flow is likely to visit a large number of unstable states and, thus, should partially equilibrate, before ending up into the laminar state. It is then plausible that the equilibrium distribution given in Eq. (10) qualitatively describes this quasiequilibrium regime. A natural assumption is that most of the paths leading to the laminar state are connected to unstable states close to $\varepsilon_{\min}(R)$, the so-called edge states in the context of turbulence. As for $R < R_g$, the average energy remains close to $\varepsilon_{\min}(R)$, the flow should reach the laminar state in a reasonably short time. Conversely, for $R > R_g$, the typical energy remains well above the threshold $\varepsilon_{\min}(R)$, and one expects that it takes a very large time to find the laminar state, as it implies excursions very far from the typical energy.

Hence, the Reynolds number R_g appears as a transition (or crossover) value between a regime of short turbulent lifetime and a regime of large lifetime. Note also that the turbulent lifetime should essentially vanish below the Reynolds value R_u where unstable states cease to exist.

B. Determination of the turbulent lifetime

In this section, we now try to put the above arguments on a more quantitative basis. We define the turbulent lifetime as the mean time to reach the laminar state after a sudden quench from a higher Reynolds number value, where turbulence is established. This situation can be modeled using Eq. (6) for the stochastic dynamics of $\varepsilon(t)$, with now an absorbing (instead of reflecting) boundary at $\varepsilon = \varepsilon_{\min}$ to account for the presence of the laminar state. The initial condition at $t = 0$ is chosen as $\varepsilon(0) = \varepsilon_{\max}$ to model the quench from high-energy turbulent states. Determining the turbulent lifetime then amounts to computing the mean first passage time at the absorbing boundary $\varepsilon = \varepsilon_{\min}$.

Such a calculation is, however, difficult for an arbitrary functional form of the entropy $s(\varepsilon, R)$ and we have to restrict the choice of $s(\varepsilon, R)$ to the linear form

$$s(\varepsilon, R) = \beta_0(R)\,[\varepsilon - \varepsilon_{\min}(R)] + s_0(R) \tag{12}$$

over the interval $\varepsilon_{\min}(R) < \varepsilon < \varepsilon_{\max}(R)$. In this case, the mean first passage time can be computed from the solution of the associated Fokker-Planck equation [88], and one finds

$$\tau = \frac{V}{D_0}\,(\Delta\varepsilon)^2\, f[V(\beta_g - \beta)\,\Delta\varepsilon] \tag{13}$$

with $\Delta\varepsilon = \varepsilon_{\max} - \varepsilon_{\min}$ and $\beta_g = \beta(R_g)$, and where the function $f(x)$ is given by

$$f(x) = \frac{1}{x^2}\,(e^x - 1 - x). \tag{14}$$

For large V, the argument of the function f in Eq. (13) is large as soon as $\beta_g \neq \beta$, that is $R \neq R_g$. The value of τ is then given, to a good approximation, by the asymptotic behavior of $f(x)$ when $x \to \pm\infty$, which reads

$$f(x) \sim \frac{1}{|x|} \quad x \to -\infty, \tag{15}$$

$$f(x) \sim \frac{e^x}{x^2} \quad x \to +\infty. \tag{16}$$

Hence, τ is given for $\beta_g < \beta$ by

$$\tau \sim \frac{\Delta\varepsilon}{D_0(\beta - \beta_g)}, \tag{17}$$

which turns out to be independent of the volume V, as intuitively expected in the large V limit. In terms of Reynolds number, one thus has a power-law divergence for R close to R_g ($R < R_g$),

$$\tau \sim \frac{\tau_0}{R_g - R}\,. \tag{18}$$

However, for any finite volume V this divergence is cut off when R approaches R_g, as soon as $R_g - R \lesssim aV^{-1}$ with some constant a, and a crossover is observed to the exponential form obtained from Eq. (16),

$$\tau \sim \frac{e^{V(\beta_g - \beta)\Delta\varepsilon}}{D_0 V(\beta_g - \beta)^2}. \tag{19}$$

Contrary to Eq. (17), expression (19) involves the volume V. For $V \to \infty$, τ becomes infinite, and a true power-law divergence is observed for $R < R_g$. Figure 4 illustrates the behavior of the turbulent lifetime as a function of β_g/β for increasing volumes. For very large but finite V, the divergence can be observed in practice only on a narrow range of Reynolds numbers before τ becomes exceedingly large. On this narrow

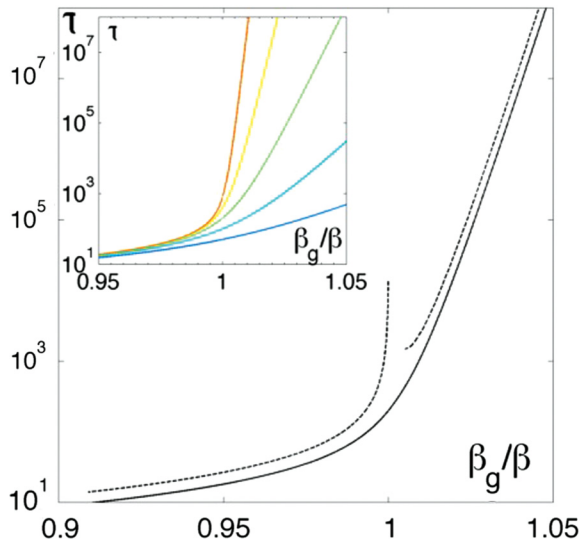

FIG. 4. (Color online) Sketch of the turbulent lifetime as a function of β_g/β, the effective Reynolds number. (Main panel) The continuous curve is the lifetime for a given volume of the system as given by Eq. (13); dashed curves are the asymptotic functional forms which govern the behavior of τ on each side of β_g; they have been shifted for clarity. (Inset) Turbulent lifetimes for increasing system size: The larger the system, the steeper the increase of lifetime. The singular behavior is observed in the limit of an infinite system size only.

range, $(\beta_g - \beta)\Delta\varepsilon$ behaves linearly with R. In contrast, if V is not too large, the range of R over which the divergence is observed broadens, and corrections to the linear behavior of $(\beta_0 - \beta)\Delta\varepsilon$ with R can become observable, possibly leading to a superexponential behavior of τ as a function of R. Though subexponential behavior cannot be discarded, one expects at least $\Delta\varepsilon$ to increase with R, which goes in favor of the superexponential case.

V. DISCUSSION

The initial motivation of the analogy proposed in this paper was twofold. First, the intense debate that animated the transition to turbulence community regarding the possible divergence of the turbulent lifetimes at a finite Reynolds number was reminiscent of a similar situation encountered in the physics of glasses a few decades earlier. Second, the idea that the dynamics is controlled by unstable solutions away from the laminar state shared some similarity with the role played by the large number of saddles at the onset of the glass transition. The goal of the analogy presented here was to make these intuitions more precise.

We have shown that, indeed, even with very good data, one cannot discriminate a singular dependence from a regular but very fast increase of the turbulent lifetimes, especially if one includes the possibility of a Vogel-Fulcher-Tammann–like singularity. We have also seen that finite-size effects may lead to a crossover, which cannot be resolved experimentally or numerically because of the extremely large time scales at play.

The model presented here was designed to be as simple as possible, taking inspiration from the random energy model with the aim to illustrate the analogy between glasses and transitional flows. As such, it does not claim to be realistic in any way, and some of its main limitations are rather obvious: The spatial structure of the flow is not taken into account, and the key ingredient (the finite slope of the entropy at minimum energy) is taken as a working hypothesis, motivated by the analogy with glasses. It is, however, quite remarkable that such a simplified model yields a crossover between a power law and an exponential form, in qualitative agreement with the experimental results. Note also that this result on the turbulent lifetime is not a straightforward mapping from the random energy model, since the latter is a purely static model, with no dynamics involved, and without any equivalent of the laminar state considered here.

These encouraging first results call for checks in direct numerical simulations of the hypotheses underlying the model. Counting the number of unstable solutions as a function of their energy density, that is, accessing $s(\varepsilon, R)$, would be a major step towards the characterization of the transition to turbulence. This is obviously a difficult task but still far less ambitious than characterizing the stability properties of these solutions and describing the complex interplay of their stable and unstable manifold. This simplification is, in essence, the gain obtained when switching from a dynamical system point of view to a statistical physics one. A first step would be to investigate a similar approach in simpler nonlinear spatiodifferential equations, where spatiotemporal intermittency has been studied, like the Kuramoto-Sivashinsky equation or the complex Ginzburg Landau one [71]. Valuable insights could also be obtained by measuring in direct numerical simulations the dissipation rate as a function of the energy density, as well as characterizing the statistical properties of the turbulent energy fluctuations in the intermediate range of Reynolds numbers.

In the above section, we have considered V as the volume of the system. However, in the spirit of real-space approaches, the relevant volume to be considered may rather be the volume of coherent regions of the flow, namely regions over which correlations extend. In a very large aspect ratio experiment, it is plausible (though not obvious) that far-away regions in the system experience no interactions. As a result, the volume V would acquire a more intrinsic nature: It would then be self-determined by the flow dynamics and not by the arbitrary size of the experiments.

Such a coherence volume cannot be accessed in the framework of models similar to the random energy model, which is mean field in nature. However, if the analogy with the physics of glasses proves to be fruitful, it would be of interest to consider its most recent developments (including, in particular, the random first-order transition scenario [89]), which precisely address the real-space description issue [44]. Pomeau [48] suggested more than twenty-five years ago that the growth and death of the laminar and turbulent regions could obey a first-order nucleation-like dynamics (albeit of a peculiar type, given the fluctuating active property of the turbulent state and the absorbing character of the laminar state). Let us conclude with the somewhat naive suggestion that taking inspiration from the random first-order transition theory of glasses might be a way to extend the standard laminar-turbulent coexistence scenario to a situation where a large number of turbulent states (associated to local unstable solutions of the Navier-Stokes equation) coexist with the laminar state.

[1] U. Frisch, *Turbulence: The Legacy of A. N. Kolmogorov* (Cambridge University Press, Cambridge, 1995).
[2] D. D. Joseph, *Stability of Fluid Motions* (Springer, Berlin, 1976).
[3] S. Grossmann, Rev. Mod. Phys. **72**, 603 (2000).
[4] O. Dauchot and P. Manneville, J. Phys. II **7**, 371 (1997).
[5] V. A. Romanov, Funkc. Anal. Prolozen **7**, 137 (1973).
[6] A. G. Darbyshire and T. Mullin, J. Fluid Mech. **289**, 83 (2006).
[7] A. P. Willis, J. Peixinho, R. R. Kerswell, and T. Mullin, Phil. Trans. R. Soc. A **366**, 2671 (2008).
[8] N. Tillmark and P. H. Alfredsson, J. Fluid Mech. **235**, 89 (1992).
[9] F. Daviaud, J. Hegseth, and P. Bergé, Phys. Rev. Lett. **69**, 2511 (1992).
[10] O. Dauchot and F. Daviaud, Phys. Fluids **7**, 335 (1995).
[11] D. R. Carlson, S. E. Widnall, and M. F. Peeters, J. Fluid Mech. **121**, 487 (1982).
[12] D. Coles, J. Fluid Mech. **21**, 385 (1965).
[13] D. Coles and C. W. Van Atta, Phys. Fluids **10**, 120 (1967).
[14] B. Hof, J. Westerweel, T. M. Schneider, and B. Eckhardt, Nature **443**, 59 (2006).
[15] T. M. Schneider, F. D. Lillo, J. Buehrle, B. Eckhardt, T. Dörnemann, K. Dörnemann, and B. Freisleben, Phys. Rev. E **81**, 015301(R) (2010).
[16] H. Faisst and B. Eckhardt, J. Fluid Mech. **504**, 343 (2004).
[17] J. Peixinho and T. Mullin, Phys. Rev. Lett. **96**, 094501 (2006).
[18] S. Bottin, F. Daviaud, P. Manneville, and O. Dauchot, Europhys. Lett. **43**, 171 (1998).
[19] S. Bottin and H. Chaté, Eur. Phys. J. B **6**, 143 (1998).
[20] A. Prigent, G. Grégoire, H. Chaté, O. Dauchot, and W. van Saarloos, Phys. Rev. Lett. **89**, 014501 (2002).
[21] A. Prigent, G. Grégoire, H. Chaté, and O. Dauchot, Physica D **174**, 100 (2003).
[22] D. Borrero-Echeverry, M. F. Schatz, and R. Tagg, Phys. Rev. E **81**, 025301 (2010).
[23] K. Avila, D. Moxey, A. de Lozar, M. Avila, D. Barkley, and B. Hof, Science **333**, 192 (2011).
[24] D. Samanta, A. De Lozar, and B. Hof, J. Fluid Mech. **1**, 1 (2011).
[25] B. Eckhardt, H. Faisst, A. Schmiegel, and T. M. Schneider, Philos. Trans. R. Soc. London A **366**, 1297 (2008).
[26] M. Lagha and P. Manneville, Eur. Phys. J. B **58**, 433 (2007).
[27] J. F. Gibson, J. Halcrow, and P. Cvitanovic, J. Fluid Mech. **611**, 107 (2008).
[28] P. Manneville, Phys. Rev. E **79**, 025301(R) (2009).
[29] D. Barkley, Phys. Rev. E **84**, 016309 (2011).
[30] D. Barkley and L. S. Tuckerman, Phys. Rev. Lett. **94**, 014502 (2005).
[31] A. P. Willis and R. R. Kerswell, Phys. Rev. Lett. **98**, 014501 (2007).
[32] T. M. Schneider and B. Eckhardt, Phys. Rev. E **78**, 046310 (2008).
[33] Y. Duguet, A. P. Willis, and R. R. Kerswell, J. Fluid Mech. **613**, 255 (2008).
[34] L. S. Tuckerman, D. Barkley, and O. Dauchot, J. Phys.: Conf. Ser. **137**, 012029 (2008).
[35] Y. Duguet, P. Schlatter, and D. S. Henningson, Phys. Fluids **21**, 111701 (2009).
[36] T. M. Schneider, D. Marinc, and B. Eckhardt, J. Fluid Mech. **646**, 441 (2010).
[37] Y. Duguet, P. Schlatter, and D. S. Henningson, J. Fluid Mech. **650**, 119 (2010).
[38] D. Moxey and D. Barkley, Proc. Natl. Acad. Sci. USA **107**, 8091 (2010).
[39] P. Manneville and J. Rolland, Theor. Comput. Fluid Dyn. **25**, 407 (2011).
[40] J. Philip and P. Manneville, Phys. Rev. E **83**, 036308 (2011).
[41] P. Manneville, arXiv:1202.0277 [physics.flu-dyn] (2012).
[42] L. Struik, *Physical Aging in Amorphous Polymers and Other Materials* (Elsevier, Amsterdam, 1978).
[43] L. Angelani, R. Di Leonardo, G. Ruocco, A. Scala, and F. Sciortino, Phys. Rev. Lett. **85**, 5356 (2000).
[44] L. Berthier and G. Biroli, Rev. Mod. Phys. **83**, 587 (2011).
[45] D. Kivelson, G. Tarjus, X. Zhao, and S. A. Kivelson, Phys. Rev. E **53**, 751 (1996).
[46] B. Derrida, Phys. Rev. Lett. **45**, 79 (1980).
[47] B. Derrida, Phys. Rev. B **24**, 2613 (1981).
[48] Y. Pomeau, Physica D **23**, 3 (1986).
[49] B. Hof, A. de Lozar, D. J. Kuik, and J. Westerweel, Phys. Rev. Lett. **101**, 214501 (2008).
[50] N. Goldenfeld, N. Guttenberg, and G. Gioia, Phys. Rev. E **81**, 035304 (2010).
[51] G. Kawahara, M. Uhlmann, and L. van Veen, Annu. Rev. Fluid Mech. **44**, 203 (2012).
[52] M. Nagata, J. Fluid Mech. **217**, 519 (1990).
[53] R. M. Clever and F. H. Busse, J. Fluid Mech. **234**, 511 (1992).
[54] A. Cherhabili and U. Ehrenstein, J. Fluid Mech. **342**, 159 (1996).
[55] S. Bottin, O. Dauchot, F. Daviaud, and P. Manneville, Phys. Fluids **10**, 2597 (1998).
[56] A. de Lozar, F. Mellibovsky, M. Avila, and B. Hof, Phys. Rev. Lett. **108**, 214502 (2012).
[57] P. Cvitanovic and B. Eckhardt, J. Phys. A: Math. Gen. **24**, L237 (1991).
[58] F. Waleffe, Phys. Fluids **9**, 883 (1997).
[59] O. Dauchot and N. Vioujard, Eur. Phys. J. B **14**, 377 (2000).
[60] B. Eckhardt and A. Mersmann, Phys. Rev. E **60**, 509 (1999).
[61] J. Moehlis, H. Faisst, and B. Eckhardt, New J. Phys. **6**, 56 (2004).
[62] J. D. Skufca, J. A. Yorke, and B. Eckhardt, Phys. Rev. Lett. **96**, 174101 (2006).
[63] J. Vollmer, T. M. Schneider, and B. Eckhardt, New J. Phys. **11**, 013040 (2009).
[64] A. Schmiegel and B. Eckhardt, Phys. Rev. Lett. **79**, 5250 (1997).
[65] T. Itano and S. Toh, J. Phys. Soc. Jpn. **70**, 703 (2001).
[66] T. M. Schneider, B. Eckhardt, and J. A. Yorke, Phys. Rev. Lett. **99**, 034502 (2007).
[67] J. Jimenez and P. Moin, J. Fluid Mech. **225**, 213 (1991).
[68] F. Mellibovsky, A. Meseguer, T. M. Schneider, and B. Eckhardt, Phys. Rev. Lett. **103**, 054502 (2009).
[69] P. Manneville, Phys. Rev. E **79**, 039904(E) (2009).
[70] J. Rolland and P. Manneville, Eur. Phys. J. B **80**, 529 (2011).
[71] K. Kaneko, Prog. Theor. Phys. **73**, 1033 (1985).
[72] H. Chaté and P. Manneville, Europhys. Lett. **6**, 591 (1988).
[73] H. Chaté and P. Manneville, in *Turbulence: A Tentative Dictionnary*, edited by P. Tabeling and O. Cardoso (Plenum Press, New York, 1994), p. 111.
[74] T. Bohr, M. van Hecke, R. Mikkelsen, and M. Ipsen, Phys. Rev. Lett. **86**, 5482 (2001).
[75] P. Grassberger and T. Schreiber, Physica D **50**, 177 (1991).
[76] P. Grassberger, J. Stat. Mech. (2006) P01004.
[77] M. Sipos and N. Goldenfeld, Phys. Rev. E **84**, 035304 (2011).
[78] F. Sciortino, J. Stat. Mech. (2005) P05015.

[79] J.-P. Bouchaud, L. Cugliandolo, J. Kurchan, and M. Mezard, *Spin Glasses and Random Fields* (World Scientific, Singapore, 1998).
[80] K. Broderix, K. K. Bhattacharya, A. Cavagna, A. Zippelius, and I. Giardina, Phys. Rev. Lett. **85**, 5360 (2000).
[81] T. S. Grigera, A. Cavagna, I. Giardina, and G. Parisi, Phys. Rev. Lett. **88**, 055502 (2002).
[82] W. van Saarloos, L. Cipelletti, J.-P. Bouchaud, G. Biroli, and L. Berthier, eds., *Dynamical Heterogeneities in Glasses, Colloids, and Granular Media*, International Series of Monographs on Physics 150 (Oxford University Press, Oxford, UK, 2011).
[83] D. Chandler and J. P. Garrahan, Annu. Rev. Phys. Chem. **61**, 191 (2010).
[84] F. Ritort and P. Sollich, Adv. Phys. **52**, 219 (2003).
[85] F. H. Stillinger, J. Chem. Phys. **88**, 7818 (1988).
[86] S. T. Bramwell, P. C. W. Holdsworth, and J. F. Pinton, Nature **396**, 552 (1998).
[87] B. Portelli, P. C. W. Holdsworth, and J. F. Pinton, Phys. Rev. Lett. **90**, 104501 (2003).
[88] S. Redner, *A Guide to First-Passage Processes* (Cambridge University Press, Cambridge, UK, 2001).
[89] J. Stevenson and P. Wolynes, J. Phys. Chem. B **109**, 15093 (2005).